

## **IDEALIZATION OF HYSTERETIC BEHAVIOR OF PRESTRESSED CONCRETE MEMBERS AND ASSEMBLAGES CONSIDERING BOND-SLIP BETWEEN PRESTRESSING STEEL AND CONCRETE**

**Masato ADACHI<sup>1</sup> And Minehiro NISHIYAMA<sup>2</sup>**

### **SUMMARY**

The authors conducted an analytical work on a prestressed concrete sub-frame assembled by post-tensioning. Layered element analysis considering bond-slip characteristics of prestressing tendon was used. The adopted parameters were the ratio of the average effective prestress to 0.2% offset yield stress of the prestressing steel and bond characteristic between the prestressing steel and concrete. The analytical results showed that the bond property had large influence on the flexural failure type of the member. Based on the analytical results, a flexural hysteresis model of prestressed concrete members was proposed. The proposed model showed better agreement with the calculated results than the idealizations proposed in the past.

### **INTRODUCTION**

Several idealizations of hysteretic load-deformation curves of prestressed concrete members have been proposed in the past. They have been used for dynamic response analyses of prestressed concrete structures. However, few of them are based on section or member properties. Load-deformation curves of prestressed concrete members vary depending on prestressing steel and non-prestressed ordinary reinforcement content, amount of prestress, location of prestressing steel in the section and bond-slip characteristic between prestressing steel and concrete. Among them bond-slip characteristic between prestressing steel and concrete is considered to have large influence on hysteresis loops of prestressed concrete members. Although bond property of prestressing steel to concrete is not so good as that of ordinary deformed bars, plane section is usually assumed in calculation of member properties such as moment capacity. Non-linear elastic load-deformation hysteresis loops, which are typical for prestressed concrete members, cannot be obtained unless poorer bond of prestressing steel than ordinary deformed reinforcement is considered.

A computer program considering bond-slip characteristic between prestressing steel and concrete was developed, to verify the influence of the bond property on the prestressed concrete members. Furthermore, a hysteresis model of prestressed concrete members is proposed based on the analytical results.

<sup>1</sup> Dept of Architecture and Architectural Systems, Kyoto University, JAPAN E-mail: adachi@rc-9500.archi.kyoto-u.ac.jp

<sup>2</sup> Dept of Architecture and Architectural Systems, Kyoto University, JAPAN E-mail: mn@.archi.kyoto-u.ac.jp

## ANALYTICAL METHOD

### Layered Element Method

For the purpose of numerical calculation, a structural member is divided into several blocks in the direction of longitudinal member axis and each block is further subdivided into layers. This method is called "Layered Element Method". In this study, the followings are assumed.

- 1) Stress and strain are constant in each layer element.
- 2) The cross section of the member remains plane after loading, i.e., the longitudinal strain in concrete is proportional to the distance from the neutral axis.
- 3) Shear deformation is not taken into account. Therefore, bending and axial forces are assumed to dominate the deformation of the member.

The outline of layered element method was described in the following section. The detail is reported by [Nishiyama, Muguruma and Watanabe, 1989].

Fig.1 shows the equilibrium of the forces around the j-th node that is between j-th and (j-1)-th element. The increment of bond stress:  $\Delta t_j$  is calculated by the following equation.

$$\Delta t_j = \frac{2 \cdot (\Delta_p \mathbf{e}_j \cdot {}_p E_j \cdot {}_p A - \Delta_p \mathbf{e}_{j-1} \cdot {}_p E_{j-1} \cdot {}_p A)}{{}_p \mathbf{y} \cdot (l_j + l_{j-1})} \quad (1)$$

where,  $\Delta_p \mathbf{e}_j$ : strain increment of tendon,  ${}_p E_j$ : tangential stiffness of stress-strain relation of tendon,  ${}_p A$ : cross sectional area of tendon,  ${}_p \mathbf{y}$ : perimeter of tendon, and  $l_j$ : longitudinal length of element.  $\Delta t_j$  is also expressed by bond-slip relationship of tendon, as follows,

$$\Delta t_j = K_j \cdot \Delta S_j \quad (2)$$

where,  $K_j$ : tangential modulus of bond-slip relation, and  $\Delta S_j$ : increment of slip. Fig.2 shows compatibility of displacements around j-th element. From Fig.2, slip increment at j-th node  $\Delta S_j$  is expressed by the following equation.

$$\Delta S_j = \Delta v_j - \Delta u_j \quad (3)$$

where,  $\Delta v_j$ : displacement increment of concrete, and  $\Delta u_j$ : displacement increment of tendon at j-th node. Elongation increment of tendon:  $\Delta_p \mathbf{e}_j \cdot l_j$  and of concrete:  $\Delta_c \mathbf{e}_j \cdot l_j$  in j-th element are calculated by Eq.4 and Eq.5, respectively.

$$\Delta_p \mathbf{e}_j \cdot l_j = \Delta u_{j+1} - \Delta u_j \quad (4)$$

$$\Delta_c \mathbf{e}_j \cdot l_j = \Delta v_{j+1} - \Delta v_j \quad (5)$$

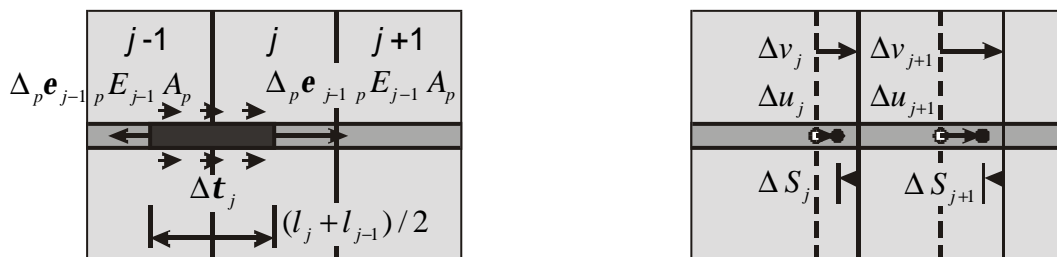


**Figure 1: Equilibrium of forces** **Figure 2: Compatibility of deformations**

From Eq.3, 4 and 5, the following equation is obtained.

$$\Delta S_j - \Delta S_{j-1} = \Delta_c \mathbf{e}_j \cdot l_j - \Delta_p \mathbf{e}_j \cdot l_j \quad (6)$$

By substituting Eq.1 and 2 into 6,  $D_p \mathbf{e}_j$  as a function of  $D_c \mathbf{e}_j$  can be obtained.

### Material property

Assumed monotonic stress-strain relationship of concrete is proposed by [Sun and Sakino, et al, 1994], whereas cyclic rule is proposed by [Watanabe, Lee and Nishiyama, 1995]. In this study, tensile stress of concrete is neglected. In addition, stress-strain curve idealization developed by [Menegotto and Pinto, 1973] for ordinary strength steel is applied to prestressing steel.

Some experimental works on bond characteristics of prestressing strand were conducted in the past, for example by [Lardji and Young, 1988](Ref.A) and by [Korenaga, Watanabe and Kobayashi, 1994](Ref.B). They carried out monotonic pullout tests on prestressing strand embedded in the concrete blocks. Furthermore, [Scribner and Kobayashi, 1984](Ref.C) conducted cyclic pullout tests. They obtained the influential tendency of some parameters, e.g. compressive strength of concrete, diameter of strand and so forth, on bond characteristic. However they did not quantitatively obtained the properties of bond characteristic, especially initial bond stiffness  $K_s$ .

In this study, two parameters, initial bond stiffness  $K_s$  and bond yield stress  $t_y$ , are chosen. In addition, bi-linear model is adopted as monotonic loading. These two properties obtained in Ref.A-C are shown in Table 1. In case that these values are not shown explicitly, the values are obtained from figures indicating bond stress-slip relation.  $t_y$  were calculated on the assumption that the perimeter of strand  $p_y$  is  $p_p f$ , where  $p_f$  is nominal diameter of strand.  $K_s$  was not obtained in Ref.C.

Although the experimental method was different, the values in Table 1 show that  $K_s = 30 - 40$  (N/mm<sup>3</sup>) and  $t_y = 3.0 - 3.5$  (N/mm<sup>2</sup>) are suitable to adopt. Moreover, bond characteristic between ordinary strength deformed bar and concrete is also shown in Table 1.  $K_s$  and  $t_y$  of prestressing strands were about 20% and 33% against those of deformed bar, respectively.

The adopted cyclic bond characteristic model of prestressing strand is proposed by [Morita and Kaku, 1975](Ref.D), which expresses the cyclic bond stress-slip relation of ordinary deformed bar. Fig.3 shows an example of bond characteristic of prestressing strand under reversed cyclic loading.

**Table 1: Initial bond stiffness  $K_s$  and bond yield stress  $t_y$  shown in Ref.A-D**

		Strand			Deformed bar
		Ref. A	Ref. B	Ref. C	Ref. D
$K_s$	N/mm <sup>3</sup>	25 - 35	40 - 60	-	196
$t_y$	N/mm <sup>2</sup>	2.5 - 3.7	3.0 - 4.8	2.0 - 2.7	9.81

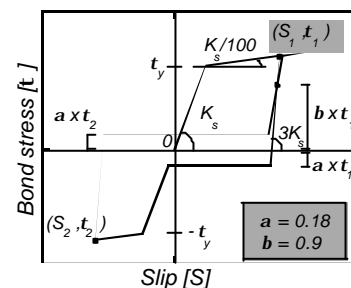


**Figure 3: Assumed bond characteristic**

### VERIFICATION BY TEST RESULTS

For verifying its propriety, the computational program was applied to precast post-tensioned beam-column joint assemblages reported by [Kono, Mimaki and Tanaka (1997)]. Fig.4 shows the overview of the test specimen. The experimental parameters were the location of prestressing strand and the existence of bond between strand and concrete. Two test units out of eight were chosen for comparison. The difference between them was the existence of bond between prestressing strand and concrete, namely B2 with bond and U2 without bond, and any other parameters such as the eccentricity of strands, material properties and the effective prestressing force were the same.

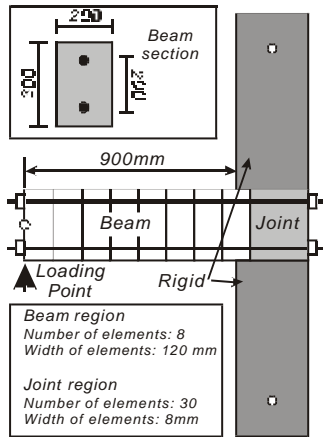


Figure 4: Test specimen

In order to compare only flexural behaviour of the beam, both experimental and analytical results neglected the flexural deformation of column. The deformation of concrete in the beam-column joint was neglected in the analysis. Fig.4 also shows block elements of the member used in the analysis.

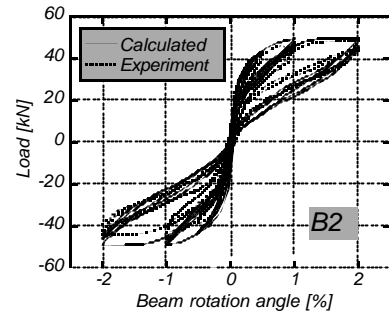
$K_s = 30.0$  (N/mm<sup>3</sup>) and  $t_y = 3.0$  (N/mm<sup>2</sup>) were assumed in B2 according to Table 1. In the case of U2, it was assumed that the bond characteristic was linearly elastic, and that the bond stiffness was small enough ( $K_s = 0.001$  (N/mm<sup>3</sup>)). The major material properties are listed in Table 2.

Fig. 5 shows the analytical results of load-beam rotation angle relationship in solid line and the experimental results in dotted line. Although the analytical results fit well against the experimental ones until the last loop ( $\theta = 2.0\%$ ) in B2, the analytical load capacity was about 10% greater than the experimental one in U2. However, small difference was observed between the analytical and the experimental results.

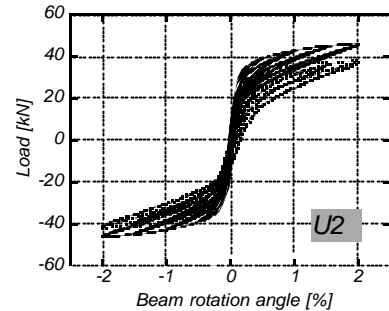
In the test, the stress fluctuation measured by load cells at the anchorage. Fig.6 shows the stress in tendon plotted against beam rotation angle at the end of beam-column joint. According to Fig. 6, the maximum tendon stress attained in the analytical result was greater than the experiment. However, in the analytical result, the stress in tendon at  $\theta = 0\%$  was almost the same with the experiment. The analytical result shows good agreement with the experimental one.

Table 2: Material properties

		B2	U2
$f'_c$	N/mm <sup>2</sup>	35.2	36.0
$s_{py}$	N/mm <sup>2</sup>	1830	
$A_p$	mm <sup>2</sup>	98.7	
$P_e$	kN	123	126
$I_P$	(Eq.7)	0.687	0.704
$I_N$	(Eq.8)	0.116	0.117
$K_s$	N/mm <sup>3</sup>	30.0	0.001
$t_y$	N/mm <sup>2</sup>	3.00	-



(a) Specimen B2



(b) Specimen U2

Figure 5: Load-beam rotation angle relation

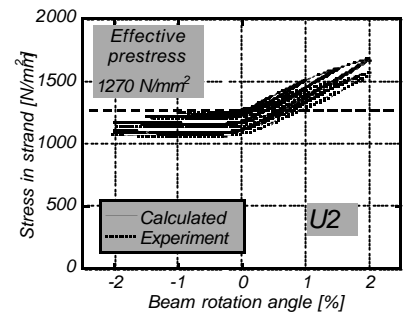


Figure 6: Stress in tendon-beam rotation angle relation

## PARAMETRIC STUDY

In order to make the relation clear between section properties and load-displacement behaviour, parametric study was conducted. The parameters to be estimated were the followings.

- 1) Section properties;  $I_P$  : the ratio of effective stress to 0.2% offset yield stress in tendon (cf. Eq. 7),  $I_N$  : the amount of prestressing force defined by Eq. 8., non-prestressed ordinary mild steel content, location of the prestressing steel in the section, and so on.
- 2) Member properties; shear span ratio, type of the frame (internal or external beam-column joint assemblages).
- 3) Bond characteristic of the prestressing steel; initial bond stiffness:  $K_s$ , bond yield stress:  $t_y$ , bond behaviour under cyclic loading.

The ratio  $I_P$  and  $I_N$  are defined as the following equations.

$$I_P = \frac{s_{pn}}{s_{py}} \quad (7)$$

$$I_N = \frac{\sum P_e}{A_g \cdot f_c'} \quad (8)$$

where,  $s_{pn}$ : effective prestressing stress,  $s_{py}$ : 0.2% offset yield stress,  $P_e$ : effective prestressing force in each prestressing steel,  $A_g$ : gross sectional area of member,  $f_c'$ : compressive strength of concrete. As  $I_P$  is close to 1.0, it is expected that the prestressing steel yields and yield region extends along the member even if bond characteristic is not good.

**Table 3: Material properties in Chap. 4**

		$I_P$ 0.4	$I_P$ 0.6	$I_P$ 0.8
$A_p$	mm <sup>2</sup>	146	97.2	72.9
$f_c'$	N/mm <sup>2</sup>	35.0		
$s_{py}$	MPa	1800		
$P_e$	kN	105		
$I_N$		0.1		

In this study,  $I_P$  and bond characteristic of the prestressing steel were adopted as parameters to examine, whereas  $I_N$  was constant ( $I_N=0.1$ ).  $I_P$  ranges 0.4, 0.6 and 0.8, which were altered by changing the sectional area of the prestressing steel:  $A_p$ . The values of  $A_p$  were shown in Table 3. Meanwhile the bond characteristics investigated were decided to simulate the bond conditions of deformed bar, of strand, and completely bonded (plane section analysis). Similar to Chap. 3,  $K_s = 30.0$  (N/mm<sup>3</sup>) and  $\tau_y = 3.0$  (N/mm<sup>2</sup>) were assumed for the bond condition of strand. In addition,  $K_s = 196.0$  (N/mm<sup>3</sup>) and  $\tau_y = 9.81$  (N/mm<sup>2</sup>) were assumed for deformed bar according to Table 1. Both  $K_s$  and  $t_y$  of a strand were smaller than those of a deformed bar.

The property of assumed member in this chapter was the same one adopted in Chap.3. Therefore, non-prestressed ordinary mild steel as longitudinal bar was not placed in the section. Two prestressing steels were arranged symmetrically with the central axis of the section. The hysteresis rules of concrete and of prestressing steel were also the same as in Chap.3. The material properties are shown in Table 3.

### Monotonic loading

The obtained load-rotation angle relations in each case were shown in Figs. 7 (a)-(c). In spite of the difference in  $I_P$ , the flexural stiffness where the bond characteristic was assumed for a strand was smaller than that for a deformed bar. Little influence of bond characteristic on the load-rotation angle relation was observed in the case of  $I_P = 0.8$ . The flexural stiffness decreased as bond resistance decreased in the case of  $I_P = 0.4$ , as expected.

In order to make the influence of the bond characteristic on flexural behaviour of PC member clear, the flexural characteristic points were defined in this study, which were cracking(Cr), yielding(Y) and flexural capacity(U). The Cr and U defined the point where the flexural crack occurred and where the load at beam end reached the flexural capacity in the calculation, respectively. So as to evaluate the point Y, two points were obtained. One was the point PY where the tensile stress of the prestressing steel reached  $s_{py}$  and the other was the point CY where the strain of the extreme compression fibre in the beam critical section reached 0.3%. As the point Y, it was adopted whichever rotation angle of the two is smaller. Table 4 shows the load and the rotation angle of every flexural characteristic point obtained in the calculation.

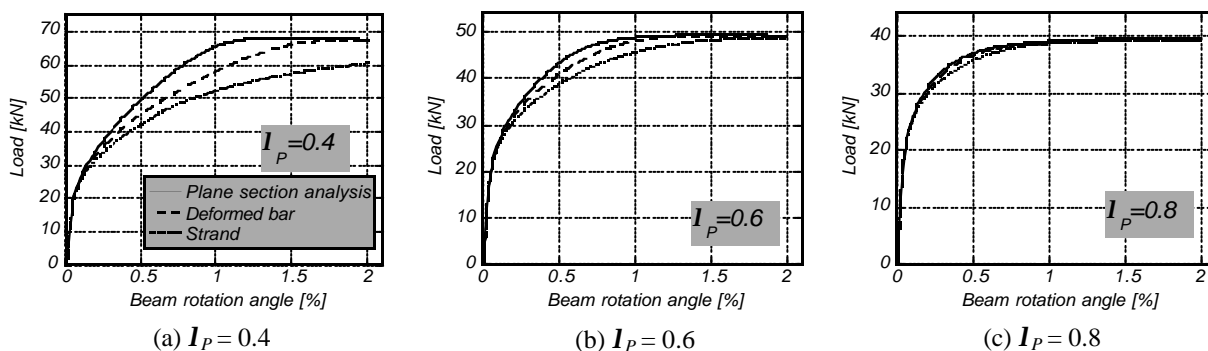


**Figure 7: Analytical results under monotonic loading**

**Table 4: Flexural characteristic points in analytical results**

		$I_p = 0.4$			$I_p = 0.6$			$I_p = 0.8$		
		P*	D	S	P	D	S	P	D	S
Cr	$P_{cr}$ kN	19.0	18.9	18.8	18.7	18.7	18.6	18.6	18.5	18.5
	$q_{cr}$ %	0.04	0.04	0.04	0.04	0.04	0.04	0.04	0.04	0.04
Y	$P_y$ kN	66.2	59.7	51.8	46.5	47.5	45.9	36.1	36.8	37.3
	$q_y$ %	1.03	1.07	0.96	0.67	0.92	1.02	0.41	0.51	0.67
U	$P_u$ kN	68.2	67.3	63.1	49.4	49.1	48.6	39.5	39.4	39.2
	$q_u$ %	1.16	1.82	3.27	1.57	1.57	1.81	1.66	1.70	1.74

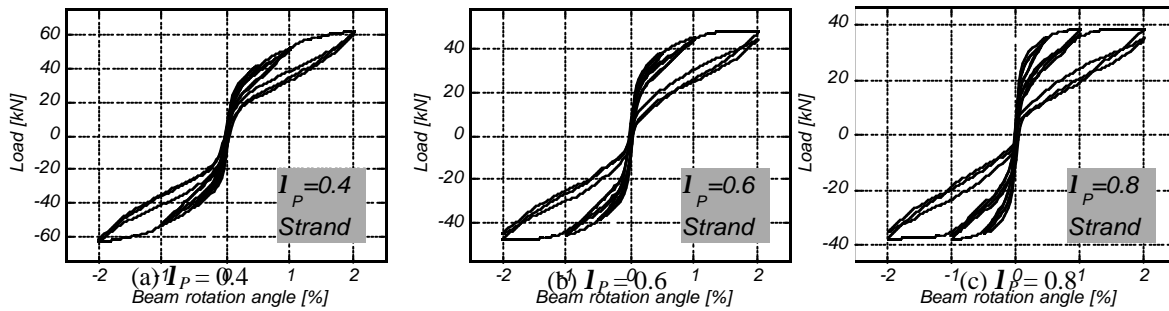
\* Type of the bond condition; P: Plane section analysis, D: Deformed bar, S: Strand

Table 4 shows that rotation angle as well as load of Cr was the almost the same in all cases in spite of the different bond characteristic. When  $I_p$  were 0.6 and 0.8, little influence of the bond characteristic on flexural capacity is observed. Meanwhile in the case where  $I_p$  was 0.4, the flexural capacity that had bond characteristic for strand was 6% smaller than that for deformed bar. This is because the type of flexure failure changed from tension failure to compression failure.

### Cyclic loading

Two cycles of loading were applied at each of the beam rotation angle of 0.5, 1.0 and 2.0%. The bond condition for strand was assumed. The load at the beam end plotted against the beam rotation angle in each case was shown in Figs.8 (a)-(c).

Figs.8 show very narrow hysteresis loop in every case, since the non-prestressed ordinary mild steel as the longitudinal bar was not placed in the section. The smaller  $I_p$  was assigned, the narrower hysteresis loops were observed. This is because the residual prestressing force was large, when  $I_p$  was small. In addition, the prestressing force was maintained even after the cycle that beam rotation angle was 2.0%, therefore the origin-oriented type of hysteresis loops did not disappear until the last loading cycle in every case.



**Figure 8: Analytical results under reversed cyclic loading**

### LOAD-ROTATION ANGLE IDEALIZATION OF PRESTRESSED CONCRETE MEMBERS

In this section, a new idealization is proposed, which is based on the idealization proposed by [Nishiyama and Watanabe, 1996]. They modified the idealization proposed by [Thompson and Park, 1980]. Both models were originally proposed for moment-curvature relation. However, load-rotation angle relation was equivalent to moment-curvature provided that the plastic hinge length was constant while loading. In this study, load-rotation angle relation of prestressed concrete members was idealized.

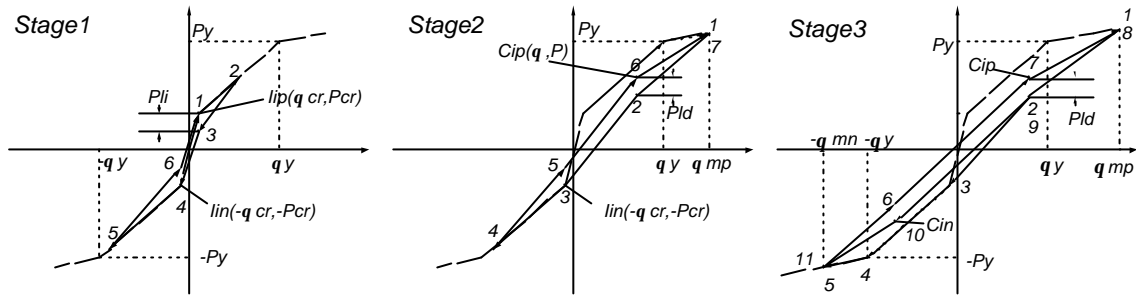


Figure 9: Nishiyama and Watanabe idealization

### Nishiyama and Watanabe idealization

Nishiyama and Watanabe developed an idealization, shown in Fig. 9, for the moment-curvature characteristics of partially prestressed concrete members under reversed cyclic loading, which covers from fully prestressed concrete to reinforced concrete members. In their idealization, the envelope curve was assumed to be tri-linear that had two turning points, which were cracking and crushing points. Figs. 10 (a)-(c) show simulated results where the condition in Sec. 4-2 was applied to Nishiyama and Watanabe idealization. In this simulation, the points Cr and Y in Table 5 were adopted as the cracking and crushing point, respectively.

As compared with Fig. 8, the simulated results show fatter hysteresis loop in the post-crushing region. The simulated flexural stiffness around the origin decreased as the deformation progressed after the crushing point. Meanwhile, Fig. 8 shows that the flexural stiffness around the origin keeps almost the initial stiffness as long as the prestressing force exists in the section.

### Modified idealization

Some modifications to the prestressed concrete idealization proposed by Nishiyama and Watanabe were made.

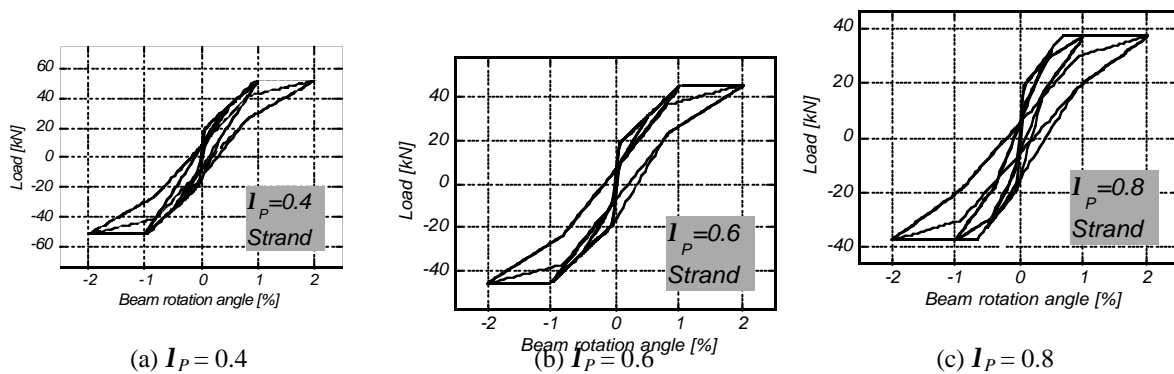


Figure 10: Simulated results based on Nishiyama and Watanabe idealization

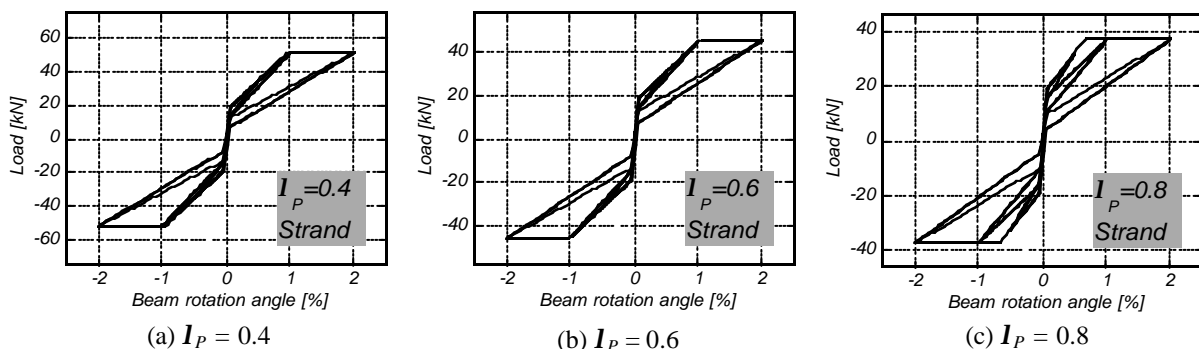


Figure 11: Simulated results based on modified idealization

In their idealization, as pointed out in Sec.5.1, the width of hysteresis loop was large a little and the flexural stiffness decreased as the deformation progressed after the rotation angle was greater than  $q_y$ . This is because the rotation angle of the point  $C_{ip}$  that was given in the Nishiyama and Watanabe model is considered too large when large curvatures are imposed on the section. Therefore, the coordinates of  $C_{ip}(q, P)$  were determined as follows,

$$P = P_{cr} \cdot (0.2 + q_y / q_{mp}) \quad (9)$$

$$q = q_{cr} \quad (10)$$

In addition, the width of the hysteresis loop was modified to  $P_{ld} / P_{cr} = 0.3 q_r / q_m$ , where  $q_r$  and  $q_m$  are the rotation angle at unloading from the envelope curve and the current value of the maximum imposed rotation angle, respectively. Fig.11 shows the simulated results of the modified idealization. They show better agreement with Fig. 8 than the original.

## CONCLUSION

- 1) Bond-slip was incorporated into a computer program that demonstrated it could pursue load-rotation angle curve obtained experimentally from a loading test on precast concrete beam-column joints assembled by post-tensioning.
- 2) Bond-slip property has a large influence on load capacity of prestressed concrete members as well as hysteresis loops.
- 3) A new load-rotation angle idealization of prestressed concrete members considering bond-slip characteristic between prestressing steel and concrete was proposed.

## REFERENCES

- Kono, S., Mimaki, Y. and Tanaka, H. (1997), "Remaining shear resistant capacity of post-tensioned beam-column connections after severe seismic loading", *Proceedings of the JCI*, Vol.19 No.2, pp.1185-1190 (in Japanese)
- Korenaga, T., Watanabe, H. and Kobayashi, J. (1994), "Bond tests on prestressing strand", *Taisei technical research report*, Vol. 27, pp.111-116 (in Japanese)
- Lardji, S. and Young, A.G. (1988), "Bond between steel strand and cement grout in ground anchorages", *Magazine of Concrete Research*, Vol.40 No.143, pp.90-98
- Menegotto, M., and Pinto, P.E. (1973), "Method of analysis for cyclically loaded R.C. plane frames including changes in geometry and non-elastic behaviour of elements under combined normal force and bending", *IABSE reports*, Vol. 13, pp.15-22
- Morita, S. and Kaku, T. (1975), "Bond-slip relationship under repeated loading", *Transaction of AIJ*, No.229, pp.15-24 (in Japanese)
- Nishiyama, M., Muguruma, H. and Watanabe, F. (1989), "Hysteretic restoring force characteristics of unbonded prestressed concrete framed structure under earthquake load", *Bulletin of the New Zealand National Society for Earthquake Engineering*, Vol.22, No.2, pp.112-121
- Nishiyama, M. and Watanabe, F. (1996), "Seismic design procedure of concrete building structures by substitute damping", *11 WCEE*, Paper No.759
- Scribner, C.F. and Kobayashi, K. (1984), "Prestressing strand bond characteristics under reversed cyclic loading", *PCI Journal*, Sep.-Oct., pp.118-137
- Sun, Y.P., Sakino, K., Watanabe, K. and Tian, F.S. (1994), "Effect of configuration of transverse hoops on the stress-strain behaviour of concrete", *Transaction of the JCI*, Vol.16, pp.49-56
- Thompson, K.J. and Park, R. (1980), "Seismic response of partially prestressed concrete", *Journal of Structural Division, Proceedings of ASCE.*, ST8, pp.1755-1775
- Watanabe, F., Lee, J.Y. and Nishiyama, M. (1995), "Structural performance of reinforced concrete columns with different grade longitudinal bars", *ACI Structural Journal*, Vol.92 No.4, pp.412-418